LASER 2 FOCUS (L2F) MEASUREMENT OF INLET AND OUTLET BOUNDARY LAYER IN THE VM 100 WINDTUNNEL

Alexandros Kessar, Jiasen Hu, Torsten Fransson
Royal institute of Technology (KTH)
Dept. of Energy Technology
Div. of Heat and Power Technology
10044 STOCKHOLM

ABSTRACT
A prerequisite for aeroelastic stability prediction in turbomachines is the understanding of the fluctuating aerodynamic forces acting on the blades. Unsteady transonic flows are complex because of mutual interactions between travelling pressure waves, outlet disturbances, shock motion, and fluctuating turbulent boundary layers. Complex phenomena appear in the shock/boundary layer region and produce phase lags and high time harmonics, which can give a significant contribution to the overall unsteady lift and torque, and therefore affect flutter boundaries, cause large local stresses, or even severely damage the turbomachine.

This paper is concerned with the experimental study of shock-boundary layer interaction in unsteady transonic flow. More precise, investigate the boundary layer characteristics at the inlet and outlet boundary to provide data for starting numerical calculations.

INTRODUCTION
Inflow boundary information are of high interest in order to characterize and understand Shock Boundary Layer Interaction. Inlet boundary layer profiles were investigated on the lower wall of the rectangular channel duct (without any test object) by Sigfrid [2003] using hotwire and PIV techniques.

At an early stage of the project, a 3D Laser-Two-Focus equipment was put into service at the division and a short measurement campaign was performed by Bron [2004] in the wind tunnel facility with the aim at determining, whether or not, the L2F technique was suitable to boundary layer measurements in such high speed flow configuration. As a result, flow velocity measurements were performed on all four walls, at both inlet (x=-90mm) and outlet (x=200mm) stations, in the rectangular channel duct. Unfortunately, as a preliminary test of the the system, the laser measurements were performed at a lower pressure level (lower density thus lower Reynolds number). These set of experiments were done without any test object as well.

With the aim at simulating realistic configurations, the test section of the VM 100 wind tunnel was instrumented with a test object, so called 2D bump which in principle represents an airfoil as it can be seen if Figure….

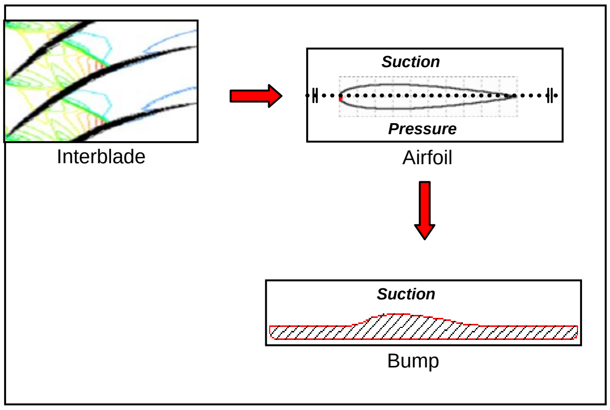

Figure 1: Modelisation of 2D bump

L2F measurements were conducted once again on all four walls, at the inlet and the outlet of the test section.

EXPERIMENTAL SET UP
The overall wind tunnel facility
The Chair of Heat and Power Technology is equipped with a 1MW compressor which can deliver a mass flow up to 4.7 kg/s at 4 bars and 30°C. A cooling system also allows a temperature adjustment from 180°C down to 30°C with an accuracy of ±0.1 degree. The flow can thereafter be redirected either into a test turbine or a conventional wind tunnel facility, as sketched on figure 1.

Stockholm, SWEDEN
September 2004

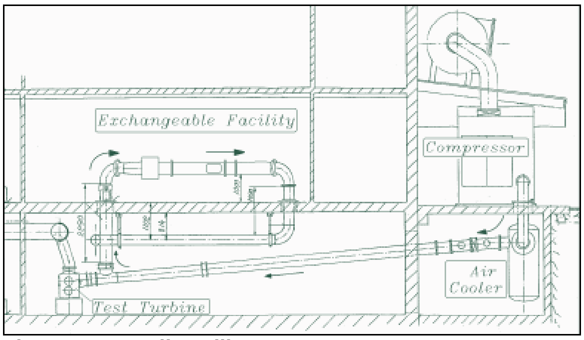

Figure 2: Overall Facility at HPT

The particularity, in the latter case, is that the test section including the settling chamber is exchangeable and allow different facilities to be inserted and investigated using the same air supply.
Another set of three valves allows to control both the mass flow and the pressure level in the test section as illustrated in Figure 3.

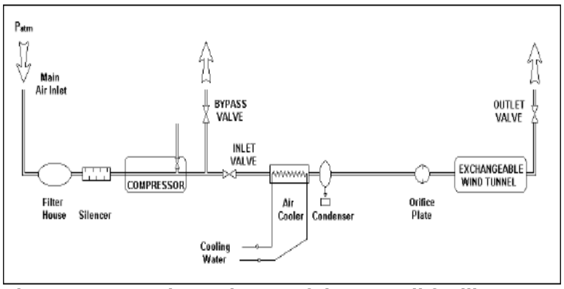

Figure 3: Operating scheme of the overall facility

By opening the inlet valve or closing the bypass valve, the mass flow can be increased inside the test section. Closing the outlet valve has the effect of increasing the pressure level and decreasing the mass flow. A sensitive set up of the different valves is necessary to adjust the mass flow and pressure level in the test section, i.e the inlet Mach number and the Reynolds number in the respective range of $Mi = 0.1 - 0.8$ and $Re = \rho_{air} U_\infty d / \nu_{air} = 1.87\ 10^4 - 1.57\ 10^6$ with $d = 0.26$m, ρ_{air}=0.54-4.48 kg/m^3 and $\nu_{air} = 1.5\ 10^{-5}\ m^2/s$. In order to compensate for the pressure losses in the different pipes between the compressor and the exhaust pipe, a fan sucks the air downstream of the test section out to the atmosphere. As a result, the pressure level can be set under atmosphere pressure when the mass flow is low.

Modular test section

The exchangeable test section of the overall facility (Fig 3) is presented in Figure 4. It features a 250mm^2 square settling chamber equipped with screens and honey combs, followed by two convergent parts which accelerate the flow into to the 120mm high and 100mm wide channel. The facility features a modular test section which can be equipped with different test objects such as bumps or flat plate. Besides, both the upper and lower walls, as well as the side walls feature large openings for optical access or instrumentation.

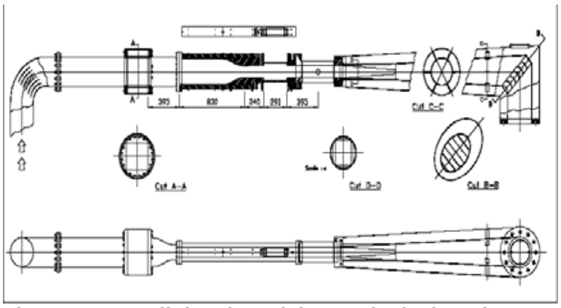

Figure 4: Overall drawing of the newly designed VM100 facility

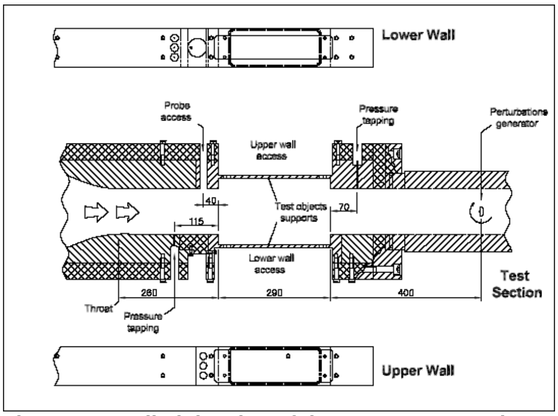

Figure 5: Detailed drawing of the VM100 test section

Measurement Technique used

After the presentation of Schodl [1980] the L2F has become a well established technique in the turbomachinery domain. It is especially suited to measure velocity and turbulence intensity in high speed and narrow flow channels. As for other laser methods, it is a non-intrusive measurement technique,that does not disturb the flow by a physical probe head. L2F was successfully applied to velocity and turbulence measurements at the RGG by Kost [1992a] and Kapteijn [1995]. A detailed review about the technique and its applications was given by Schodl [1986].

A two-dimensional L2F is able to detect velocity components in the axial and circumferential direction (x and Φ coordinates). The measuring principle for two-dimensional measurements is presented in Fig. 6. It shows the measurement volume, consisting of two focused laser beams being generated by the L2F device and working as a light gate.

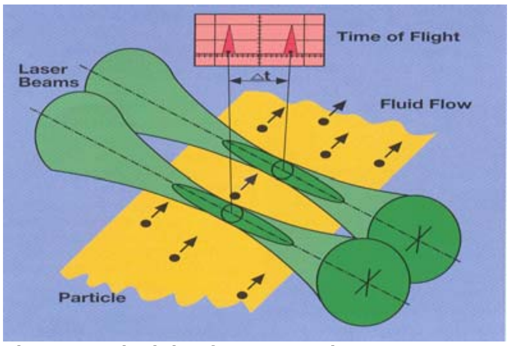

Figure 6: Principle of L2F operation

Small oil droplets are injected into the flow at an upstream position from a seeding generator. A particle passing through both foci scatters light. The two distinct light impulses are received by photo detectors. The distance between both foci, s, (for the presented 3D-L2F measured to 280 $\pm$ 0.3 μm) is known and the time delay between the two impulses, the time-of-flight (TOF), is measured. Thus the particle velocity can be calculated.

To ensure that in fact the same particle travels through both foci a high number of TOF must be measured. The second focus point is rotated around the first one to detect the main flow orientation in the plane being normal to the optical axis. A complete measurement at one point consists of the stepwise rotation of the stop focus around the start focus. Typical number of steps are 11-21 with a step distances of 0.72° - 1.44°, both depending on the turbulence intensity. At every angular step a number of measurements is carried out, based on a pre-selected number of particles passing the start focus (usually 5000). Not all of these 5000 start impulses result in successful TOF measurement. However, a TOF distribution for each angular step is obtained. By statistical data treatment of the obtained probability density distributions the mean velocity magnitude $|\vec{c}|$, the flow angle α and the turbulence intensities parallel and vertical to the main flow direction are calculated.

The 3D-L2F consists of two two-dimensional systems observing the same measurement volume from different angles of incidence. Fig. 7 displays the principle of operation with the two single systems, called channel 1 and channel 2. The two pairs of beams rotate around the optical axis. The angle between the main flow direction and a zero position, what is normally orientated horizontally, is the finally obtained flow angle α. In case of velocity vectors perpendicular to the optical axis (2D flow) the two channels behave as standard L2F systems. However, if the velocity has a radial component, the system can be rotated that such an arbitrary vector $\vec{c}$ lies just within the plane defined by start and stop focus of channel 1. A flow angle $\alpha_{channel1}$ is detected. Channel 2 does not see correlated time-of-flight signals. A small turning of the system around the optical axis will bring $\vec{c}$ into the plane defined by start and stop focus of channel 2. Now correlated time-of-flight events are detected in channel 2, but not in channel 1. This results in a flow angle $\alpha_{channel2}$. The final flow angle α is calculated to:

$$\alpha = \frac{1}{2}\left(\alpha_{channel1} + \alpha_{channel2}\right)$$

Eq. 1

The 3D velocity magnitude is obtained from the two 2D velocity and angle results. γ is the inclination angle of both channels to the optical axis

$$|\vec{c}| = \frac{\frac{1}{2}\left(|\vec{c}_{channel1}| + |\vec{c}_{channel2}|\right)}{\cos\left(\frac{1}{2}\left(\alpha_{channel2} - \alpha_{channel1}\right)\right)\cdot\cos\gamma}$$

Eq. 2

The radial flow angle χ is defined to be zero perpendicular to the optical axis and being positive in direction towards the collimator lens. It is calculated according to:

$$\chi = \mathrm{atan}\left[\frac{\sin\left(\frac{1}{2}\cdot\left(\alpha_{channel2} - \alpha_{channel1} + \Delta\alpha_0 - \Delta\alpha_{grad}\right)\right)}{\tan\gamma}\right]$$

Eq. 3

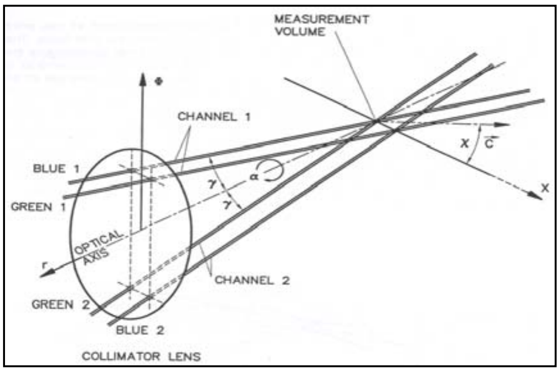

Figure 7: Principle of operation of 3D L2F

The difference of the measured $\alpha_{channel2}$ and $\alpha_{channel1}$ is usually small. This requires very accurate measurements of $\alpha_{channe1}$ and $\alpha_{channel2}$ to obtain satisfactorily accurate values for the radial flow angle χ. This is ensured by a calibration, described by Maass et al. [1994], resulting in the coefficient $\Delta\alpha_0$. It provides the exact inclination angle γ and compensates inexact axial focus positions. $\Delta\alpha_{grad}$ compensates undesired influences from gradients of the flow angle α in circumferential direction (along Φ-coordinate) direction across the measurement volume.

Fig. 8 provides an impression of the 3D-L2F optical head. The realised technical solution works with two separated collimator lenses, but the principle of operation is identical to the one described above.

Figure 8: Optical head of the 3D L2F

According to Schodl [1980] particles of a diameter of not more than 0.3 μm are required to follow the flow almost instantaneously, also over shock waves. For the present experiments Diethylhexylsebacat (DEHS, $C_{26}H_{50}O_4$), a non-flammable, non-toxic oil substance was used. The particle mean diameter was 0.08-0.1 μm. The percentage of particles being larger than 0.3 μm was very small [Polytec, 1997b].

The measurement position is reached by a software controlled three-dimensional traverse system. The measurement volume is moved in axial and radial position by this traverse. The circumferential position relative to the stator vanes is changed by rotating the stator, while the measurement volume is kept constant.

RESULTS

Vertical and horizontal traverses were performed using the L2F system at both inlet and outlet, in the center of the rectangular channel duct for three different operational conditions:

Ptin = 160kPa, Ptout = 106 kPa, Min = 0.702

Ptin = 160kPa, Ptout = 110 kPa, Min = 0.692

Ptin = 160kPa, Ptout = 118 kPa, Min = 0.642

The measurement campaign was divided into three different segments as the laser had to be inclined upwards and downwards by 10^0. Horizontal, upper part and lower part. By doing so, the laser was able to perform measurements up to 1mm away from the bottom and upper wall. In the photo that follows, it shows how this division of the measurement campaign was done.

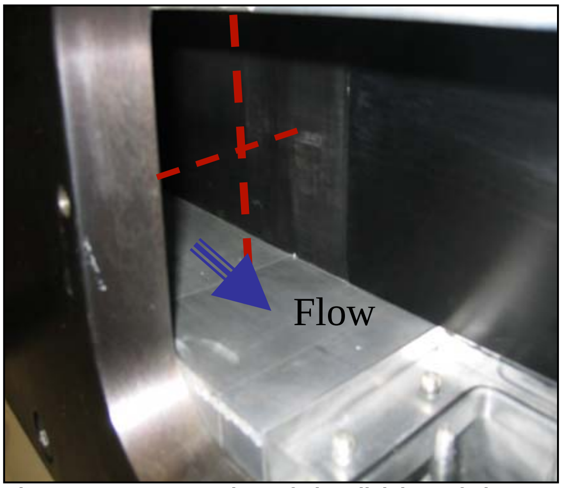

Photo 1: Representation of the division of the test section

The boundary layer profiles were then extracted and are presented in figures 9-11.

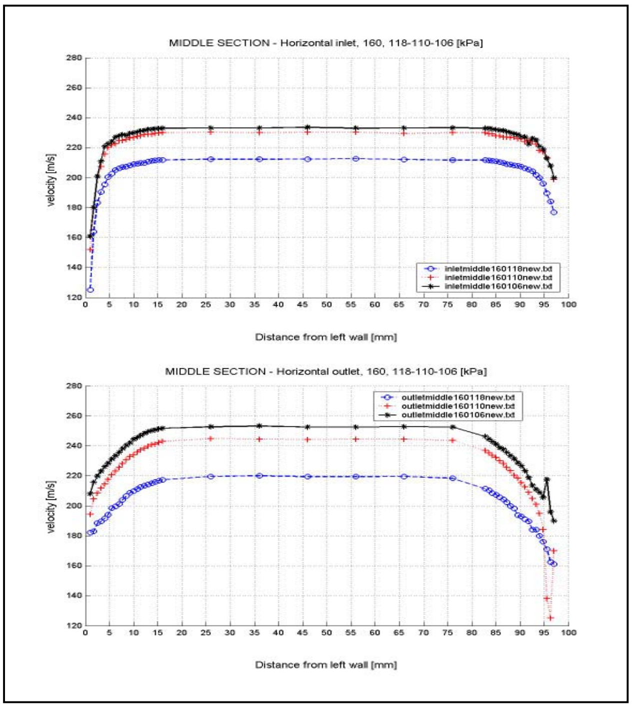

Figure 9: Middle section

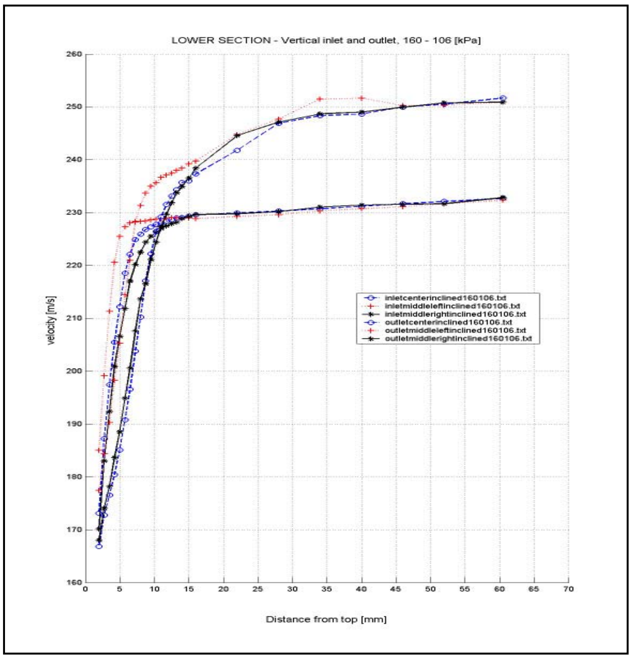

Figure 10: Lower section

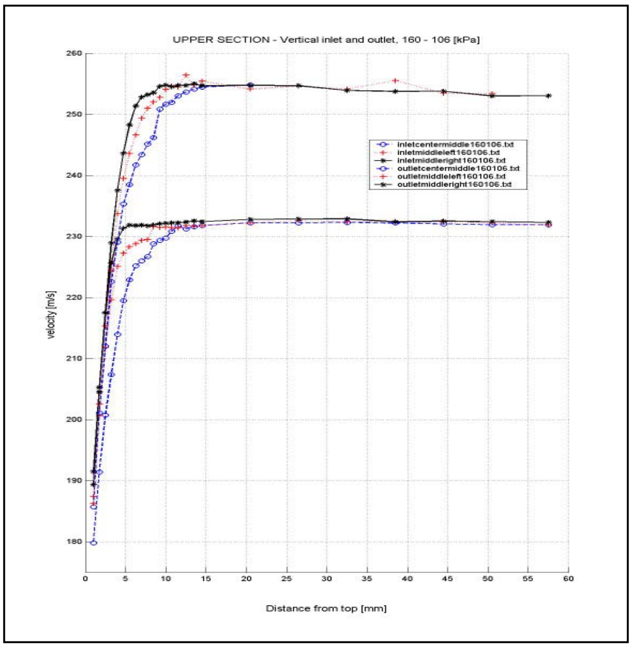

Figure 11: Upper section

From L2F measurements, it appears that the BL on the lower wall at the inlet of the test section, without any test object, is about 12mm thick whereas the BL on all other walls are slightly thinner (10 to 11mm thick). On the contray, when the 2D bump is included then, as it is obvious form the graphs as well, the thickness of the boundary layer increases considerably on all the walls around the duct. These results are summarized in the tables that follow:

	Inlet	Outlet
Lower wall	11.5 mm	14 mm
Upper wall	10.2 mm	11 mm
Right side	10 mm	21 mm
Left side	10.5 mm	19 mm

Old experimental boundary layer characteristics without test object, Bron [2004]

	Inlet	Outlet
Lower wall	14 mm	25 mm
Upper wall	14 mm	15 mm
Right side	10 mm	23 mm
Left side	16 mm	25 mm

Experimental boundary layer characteristics with 2D bump

The dissymmetry in the in-flow BLs could originate a general non uniformity in the incoming flow field or simply the dual contraction design. Indeed, the two small settling chamber probably does not fully dissipate the flow gradients originating the last corner of the pipe system. In addition, the double contraction design certainly has an influence on the dissymmetry between side wall BLs and the other BLs. Observing the behaviour of the different BLs between the inlet and outlet stations, it is noteworthy that the BLs on the side walls thicken much more than on the upper and lower walls. As seen in Figures 1-6, it is actually difficult to tell where exactly the edge of the side wall BLs is located at the outlet. Indeed, the thickening of all BLs is equivalent to a narrowing of the effective section area and the flow slightly accelerates in the free stream, which induces a continuous increase of the velocity on the side wall BLs.

CONCLUSIONS

A L2F experimental study has been performed in a transonic wind tunnel to investigate the boundary layer characteristics upstream and downstream of a 2D bump. The measurement shows that the L2F technique can work well in the present experimental campaign. The thickness of the boundary layer on all the walls, when the 2D bump is equipped, increases considerably compared with the measurements without the bump in test section. The present experimental data, together with the pressure measurements on the bump (Bron, 2004) provide a complete test case for the numerical investigation of shock-boundary layer interaction

REFERENCES

Schodl, R; 1980
"A Laser-Two-Focus (L2F) Velocimeter for Automatic Flow Vector Measurements in the Rotating Components of Turbomachine"
J. Fluid Eng., Vol. 102, pp. 412-419, 1980.

Schodl R; 1986
"Laser – Two – Focus Velocimetry"
Advanced Instrumentation for Aero Engine Components, AGARD CP-399, 198

Kapteijn, C.; 1995
"Wake Development Downstream of a Transonic Turbine Inlet Guide Vane with Trailing Edge Ejection."
AGARD CP-571: "Loss Mechanisms and Unsteady Flow in Turbomachines.", Derby, 1995

Kost, F., 1992a
"Three Dimensional Transonic Flow Measurements in an Axial Turbine with Conical Walls."
ASME Paper No. 92-GT-61, 1992

Freudenreich, K.; 1998c
"Time-dependent Laser Measurements in Turbomachinery Applications - Physical Background and Measuring Techniques."
Literature Study and Internal Report KTH/HPT 98/32, Chair of Heat and Power Technology, Department of Energy Technology, Stockholm, Sweden, foreseen for 1998

Freudenreich, K.; Fransson, T. H.; 1998
"Application of Three Dimensional Laser-Two-Focus Anemometry to Transonic Turbine Flows: Example of an Isolated Stator."
14th Symposium on Measuring Techniques for Transonic and Supersonic Flow in Cascades and Turbomachines, Sep. 2-4, University of Limerick, Ireland, 1998

Maass, M.; Förster, W.; Thiele, P.; 1994
"Unsteady Flow Experiments in the Exit of a Ducted Propfan Rotor."
AIAA Paper No. 94-2970, 1994

Polytec; 1997a
"Manual for the L2F-O-6000."
Polytec GmbH, Waldbronn, Germany, 1997

Polytec; 1997b
"Manual for the particle generator L2F-1000A."

Bron, O., 2004

Sigfrid, N., 2004